Applied Clay Science 143 (2017) 125–133

Contents lists available at ScienceDirect

Applied Clay Science

journal homepage: www.elsevier.com/locate/clay

Research paper

Fabrication, microstructural and mechanical characterization of Luffa Cylindrical Fibre - Reinforced geopolymer composite

Mazen Alshaaer[a,b,*], Saida Abu Mallouh[c], Juma'a Al-Kafawein[d], Yasair Al-Faiyz[d], Tarek Fahmy[a], Abderrazek Kallel[e,f], Fernando Rocha[b]

[a] Plasma Technology and Material Science Unit (PTMSU), Department of Physics, College of Science and Humanitarian Studies, Prince Sattam bin Abdulaziz University, Alkharj, Saudi Arabia
[b] Geobiosciences, Geotechnologies and Geoengineering Research Center, Campus de Santiago, University of Aveiro, Aveiro 3810-193, Portugal
[c] Hamdi Mango Center for Scientific Research, The University of Jordan, Amman, Jordan
[d] Department of Chemistry, King Faisal University, Al-Hassa, Saudi Arabia
[e] Department of Civil Engineering, College of Engineering, Prince Sattam bin Abdulaziz University, Alkharj, Saudi Arabia
[f] Université de Tunis El Manar, Ecole Nationale d'Ingénieurs de Tunis, LR03ES05 Laboratoire de Génie Civil, 1002 Tunis, Tunisia

ARTICLE INFO

Keywords:
Geopolymers
Kaolin
Luffa Cylindrical Fibre
Composite
Aluminosilicate

ABSTRACT

This study reports on the preparation, microstructure, density and mechanical properties of new geopolymer composites (LG-composite) that are unidirectionally and randomly reinforced with 10 vol% natural Luffa Cylindical fibres (LCF). The geopolymer matrix was synthesized from metakaolin activated with sodium silicate and sodium hydroxide solutions. A greater amount of geopolymer gel was formed after introducing the LCF into the geopolymer matrix. As a result of the strong alkali setting reactions (geopolymerization), the hemicelluloses and lignin present in the LCF were extracted, leaving a rough LCF surface. In this way the hydrophobicity of the rough LCF increased and helped strengthen the bonding between fibre and geopolymer matrix. Two main morphological types of crystalline objects were observed in the LG-composite due to the incorporation of the extracted constituents of LCF: fibre-like crystals, or whiskers, and fine crystals of cubic shape. These crystals assist in crack healing while increasing the tensile strength and toughness of the composite. In terms of mechanical properties, it is found that by introducing LCF as reinforcement, the compressive and flexural strengths of the end geopolymeric products respectively increase from 13 MP and 3.4 MPa up to 31 MPa and 14.2 MPa. The LCF-reinforced geopolymer composite exhibited ductile-like failure with a strain hardening Modulus of 72 MPa, unlike the brittle matrix. In addition, the bulk density decreases from 1.5 g/cm^3 to 1.38 g/cm^3. A preliminary aging study has demonstrated that the LG-composite shows no significant deterioration in mechanical performance over a duration of 20 months.

1. Introduction

Composite materials with high mechanical performance have received much attention in recent years (Alomayri et al., 2014). These materials cannot always be synthesized by conventional monolithic brittle ceramics or cement (MacKenzie and Welter, 2014) because they have poor tensile and flexural properties. One solution to this problem is to use an inorganic matrix, such as a ceramic or cement, in combination with fibres to overcome the problem of brittle failure and produce a more acceptable failure mode (Nematollahi et al., 2014; Assaedi et al., 2015). Since ceramics require high processing temperatures, they can be prepared only in combination with inorganic fibres. Furthermore, the high cost and the special requirements needed for ceramic processing are valid reasons for proposing other similar materials involving low cost processing and simple preparation methods (Hung et al., 2008; El-Eswed et al., 2017; Komnitsas et al., 2013).

Although ordinary cements have good mechanical properties, there may be limitations regarding their adequacy for some applications in the construction field. For example, the surface deterioration of concrete due to the chemical attack of some liquids causes a serious problem for its durability (Pernica et al., 2010). Moreover, increasing awareness of greenhouse emissions resulting from Portland cement manufacturing makes it necessary to look for an alternative “green” material —around 5% of global CO_2 emissions arise from Portland cement production (Huntzinger and Eatmon, 2009), and studies (Roy, 1999; Alzeer and MacKenzie, 2013) indicate that producing 1 ton of

* Corresponding author.
E-mail address: mazen72@yahoo.com (M. Alshaaer).

http://dx.doi.org/10.1016/j.clay.2017.03.030
Received 22 January 2017; Received in revised form 19 March 2017; Accepted 20 March 2017
Available online 27 March 2017
0169-1317/

ordinary Portland cement entails emitting approximately one ton of CO_2.

A new class of alternative matrix materials that are free of such drawbacks can be found in geopolymers (Roy, 1999; Barbosa et al., 2000; Huntzinger and Eatmon, 2009; Alzeer and MacKenzie, 2013). The curing, setting and hardening of these inorganic compounds occur at low temperature. Subsequently, a low-temperature ceramic-like matrix is formed with the typical temperature resistance and strength of ceramics (Komnitsas et al., 2007; Alshaaer, 2013; Hajjaji et al., 2013; Alshaaer et al., 2014). Processing geopolymers at low temperatures makes them suitable as matrices for a wide range of fibres, including organic fibres (Kriven et al., 2003). At the same time, since their production entails much lower CO_2 emission —approximately 62%–66% of that of Portland cement (Davidovits, 2015)— they are considered green cements (Duxson et al., 2007; Essaidi et al., 2014).

The geopolymer microstructure comprises an amorphous, three-dimensional network resulting from the reaction of either geological mineral or industrial wastes with an alkali silicate solution. Several studies (Davidovits, 1982, 2005; El- Eswed et al., 2009; Zaharaki et al., 2010) have explored the kinetics of this reaction and identify the solution chemistry, and a reaction pathway for geopolymerization involving polycondensation of hypothetical monomers, i.e. orthosialate ions, has been proposed by Davidovits (2005). Hard and stable materials with three-dimensional networks, similar to hydroxysodalite, feldspathoid or zeolite, are formed due to these reactions (Alshaaer et al., 2002). The amorphous or microcrystalline materials produced are composed of SiO_4 and AlO_4 tetrahedra linked alternately by sharing all the oxygen atoms. When aluminum is four coordinated to oxygen atoms, a negative charge is created; therefore, the presence of cations such as Na^+ and K^+ is essential to balance the negative charge of Al in the fourfold coordination (Davidovits, 1982). Despite the promising mechanical properties of geopolymers, the material's matrix is characterized by brittle failure readily taking place under applied force. Therefore, applications of this material in construction technology will benefit significantly from an enhancement of the mechanical properties such as flexural strength and toughness. This goal may be accomplished by developing “environment-friendly materials” through the use of natural fibres in a fibre-reinforced geopolymer composite (Nematollahi et al., 2014).

In principle, the advantages of using natural fibres in composites include low density, high flexural strength, flexibility and high elastic modulus (Ferreira et al., 2010; Davidovits, 2011; Bohlooli et al., 2012; Assaedi et al., 2015). Further advantages derive from the biodegradable, renewable and recyclable nature of natural fibres (Hammell et al., 2000; Assaedi et al., 2015, 2016). Based on these characteristics, natural fibres become an attractive reinforcement for composite systems. For instance, cellulose, cotton fibres, bamboo and flax are utilized to improve the mechanical performance of various composite systems (Low et al., 2009; Rahman et al., 2011).

This study aims to develop LCF-geopolymer composites with attractive physical and mechanical properties. The sponge gourd, the fruit of LCF, has a ligneous netting system in which the fibrous cords are disposed in a multidirectional array, forming a natural mat. Previous studies by Gianpietro et al. (2000), NagarajaGanesh and Muralikannan (2016), Seki et al. (2012), and Akhtar et al. (2003) involved LCF composed of 60% cellulose, 30% hemicellulose and 10% lignin. In this study, XRD and SEM were used to investigate the chemical composition, morphology and microstructure of geopolymer/LCF composites.

2. Experimental

2.1. Materials

Geopolymer cement was prepared using kaolinitic soil from natural deposit, as well as sodium silicate (Na_2SiO_3) and sodium hydroxide. The kaolinitic soil sample was collected from a deposit in Riyadh region (Saudi Arabia) with the assistance of Saudi Ceramic Company. The estimated kaolinite mass percentage in the precursor is 92%.

Table 1
Chemical analysis of kaolinite.

Compound	Composition%
MnO	0.3
Cr_2O_3	0.4
CaO	1.1
K_2O	0.1
P_2O_5	0.9
Fe_2O_3	9.3
Al_2O_3	22.5
SiO_2	38.1
TiO_2	14.2
LOI	13.1

The powdered clay (grain size less than 60 μm) was heated at 750 °C for 4 h in a laboratory furnace to obtain its respective metakaolinite. The chemical composition of the sample was determined by X-ray Fluorescence (XRF) (Bruker System S4 Pioneer) and is given in Table 1.

Sodium silicate (Na_2SiO_3) and sodium hydroxide (NaOH) solutions were used as alkaline activators for the dissolution of aluminosilicate phases. The sodium silicate solution (Merck, Germany) contained 27% SiO_2 and 8% Na_2O. The hydroxide solution, at a concentration of 6 M, was prepared using sodium hydroxide (NaOH) (Merck) and distilled water.

The luffa sponge, Fig. 1A, was obtained from dried fruits of Luffa Cylindrical Fibre (LCF). Only the outer core was used as the natural fibre matting. The homogeneous outer core of the sponge was cut into layers of fibre. The obtained fibre mats were washed with distilled water and dried at 80 °C during 24 h. Each fibre mat has two different sides: one is made up of unidirectional fibres as shown in Fig. 1B, while random fibres exist on the other side of the same mat, as in Fig. 1C.

2.2. Preparation of geopolymer cement

The ratios used during the alkaline activation process were: SiO_2 (in sodium silicate solution)/Al_2O_3 (in metakaolinite) molar ratio of 1, and Na_2O (in sodium silicate and NaOH solutions)/Al_2O_3 (in metakaolinite) molar ratio of 1. The H_2O/Na_2O molar ratio was 13. The solution of Na_2SiO_3, NaOH and H2O was mechanically mixed for 1 min. Metakaolinite was mixed with this alkaline solution for 15 min. The mixture was poured into a polycarbonate mold (16 cm × 10 cm × 2 cm), and then the mold was sealed and cured at 40 °C for one day. The geopolymer specimen was cut into smaller pieces (16 cm × 2 cm × 2 cm) using a diamond saw.

2.3. Preparation of LCF-reinforced geopolymer composite (LG-composite)

Laminates in this work were fabricated by means of the hand lay-up technique, illustrated in Fig. 2. The dimensions of each laminate are 16 cm × 10 cm × 1 cm. The amount of geopolymer used per layer was 56 g/(16 cm × 10 cm). Ten LCF mats (2D) with a fibre density of 4 g/

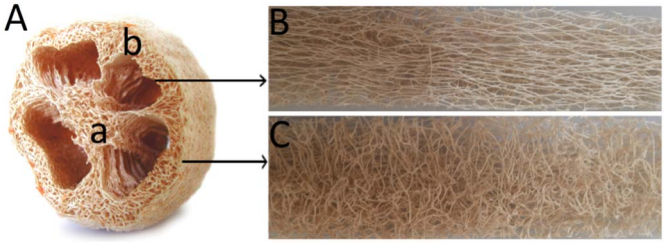

Fig. 1. The LCF fruit (A), the inner fibre core (a) and the outer core (b), unidirectional fibre (B), and random fibre (C).

(16 cm × 10 cm) were used as reinforcement. The average LCF diameter was around 200 μm. The length of the chopped fibres was 160 mm. The volume percentage of the LCF is 10% *V*/V from the total volume of the laminate.

The laminate was pressed gently using a silicone pressure roller upon the polycarbonate mold (16 cm × 10 cm × 2 cm), which was cured in a ventilated oven at 40 °C for one day after sealing the mold. After curing, the laminate was removed from the molds and cooled at room temperature. The laminate was cut into specimens (16 cm × 2 cm × 2 cm) using a diamond saw (curing and dimensions of specimens similar to SKG, section 2.2).

2.4. Mineralogical and microstructural analyses

X-ray diffraction (XRD) analyses were carried out on powdered samples to identify major crystalline and potentially newly formed phases using a Shimadzu diffractometer-6000 (Japan) with a Co tube and a scanning range from 5° to 80° 2θ at a scan rate of 2°/min. The morphology of the specimens was studied using an Inspect F50 scanning electron microscope (The Netherlands). The samples were pre-coated with platinum under an argon atmosphere. Energy-dispersive X-ray spectroscopy (EDX) was used for elemental analysis and chemical characterization of samples.

2.5. Mechanical and physical characterizations

The fabricated specimens for each series were tested for bulk density, flexural strength, compression strength, and stress-strain curves. For bulk density measurements, specimens after curing were weighed using an electronic balance and their dimensions were measured using a digital micrometer. Afterward the bulk density was calculated by dividing mass by volume.

The specimens were tested in three-point bending and in compression. Testing was performed at room temperature with a universal testing machine (Instron 5582, UK). The bending specimen's dimensions were: height = 2 cm, width = 2 cm and length = 16 cm; the distance between the supports was 120 mm, and the speed of the machine head during testing was 0.1 mm/min. Compression tests were performed on the failed bending specimens, placed on their side with a loading area = 2 × 2 cm^2 and height = 4 cm. The speed of the machine head during testing was 2 mm/min.

The flexural strength (F_r) was determined using the following equation (Alomayri et al., 2013):

$$F_r = \frac{3}{2}\frac{P_m S}{BW^2}$$

where P_m is the maximum load (N) at crack extension, S is the span of the sample, B is the specimen width and W is the specimen thickness (depth). A schematic diagram of the research methodology is illustrated in Fig. 2.

Values of the flexural modulus (E_F) were computed using the initial slope of the stress-strain curve (Alomayri et al., 2013). The strain hardening modulus is the slope of the stress versus strain curve after the point of yield of a material. Compressive strength (Fc) was calculated using the following formula:

$$F_c = \frac{P_C}{A}$$

where P_c is the maximum load (N) at failure, and A is the cross-section area of the specimen (mm^2). Bulk density (D_B) was calculated using the formula:

$$D_B = \frac{m}{V}$$

where m is the mass (g), and V is the volume of the specimen (cm^3).

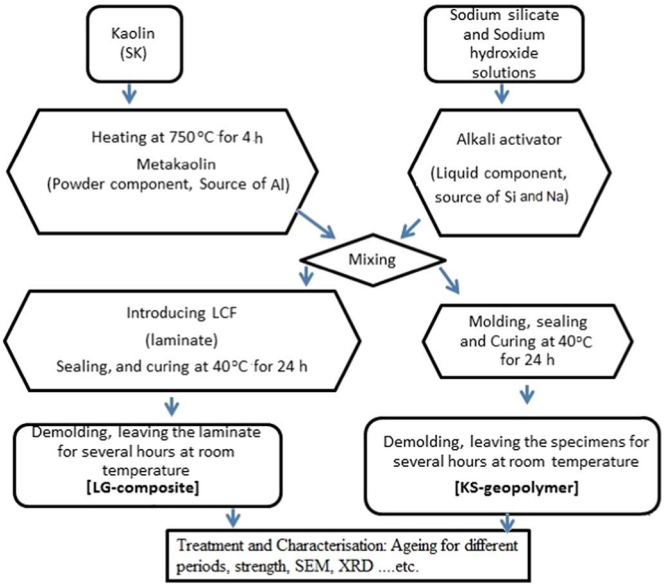

Fig. 2. The schematic diagram of the research methodology.

3. Results and discussion

3.1. Microstructural characteristics

LCFs feature a network system in which the fibrous cords appear in a multidirectional array forming a natural mat, as reported in Fig. 1. The diameter of LCF varies from 100 μm to 400 μm (Fig. 3A). Each LCF has a fibrous vascular system (Fig. 3B) composed of fibrils, around 10 μm in diameter, glued together with natural resinous materials of plant tissue. The main chemical constituents of luffa are hemicellulose, cellulose and lignin (Akhtar et al., 2003). Cellulose and hemicellulose exist in the form of hollow cellulose in LCF, representing about 82% of the total chemical constituents (Fig. 3B). Another important chemical constituent present in LCF is lignin: this component is considered a binder for the cellulose fibres and also behaves as an energy storage system (Innocent et al., 2013).

LCFs are hydrophilic in nature, absorbing moisture from the air (Parida et al., 2015). This characteristic of the LCF leads to weak adhesion with the geopolymer matrix, ultimately causing debonding between the two. In wet conditions, therefore, such composites show very low mechanical properties (Ray et al., 2001). In this study, as a result of the strong alkali setting reactions (geopolymerization), the hemicelluloses and lignin present in the LCF could be extracted. In this way the number of –OH groups present in the fibre was reduced. The decrease in –OH groups, together with the increase in hydrophobicity of natural fibres, facilitated a strengthened bonding between fibre and geopolymer matrix (Joseph et al., 2000). Geopolymerization also leads to a breaking down of the composite fibre bundle into smaller fibres, as reported in Fig. 3D (point a). It furthermore reduces LCF diameter and thereby increases the aspect ratio (width/height) which gives rise to the formation of a rough surface topography, Fig. 3C, that results in better fibre-geopolymer matrix (point b) interface adhesion. Accordingly, we assume no need for pre-alkali treatment of LCF before using them in LG-composite.

The XRD patterns of the precursor, kaolinite, and of the geopolymeric matrix (SK-geopolymer) are displayed in Fig. 4. The XRD pattern, Fig. 4A, illustrates that kaolinite also contains some anatase (TiO_2) mineral, in this case 14.2%, as reported in Table 1. As a result of kaolinite calcination and the subsequent geopolymerization, most of the crystalline phases disappear, the thermal treatment leading to dissolution in the alkaline environment, as illustrated in Fig. 4B.

SEM analysis of metakaolin and its transformation to the geopoly-

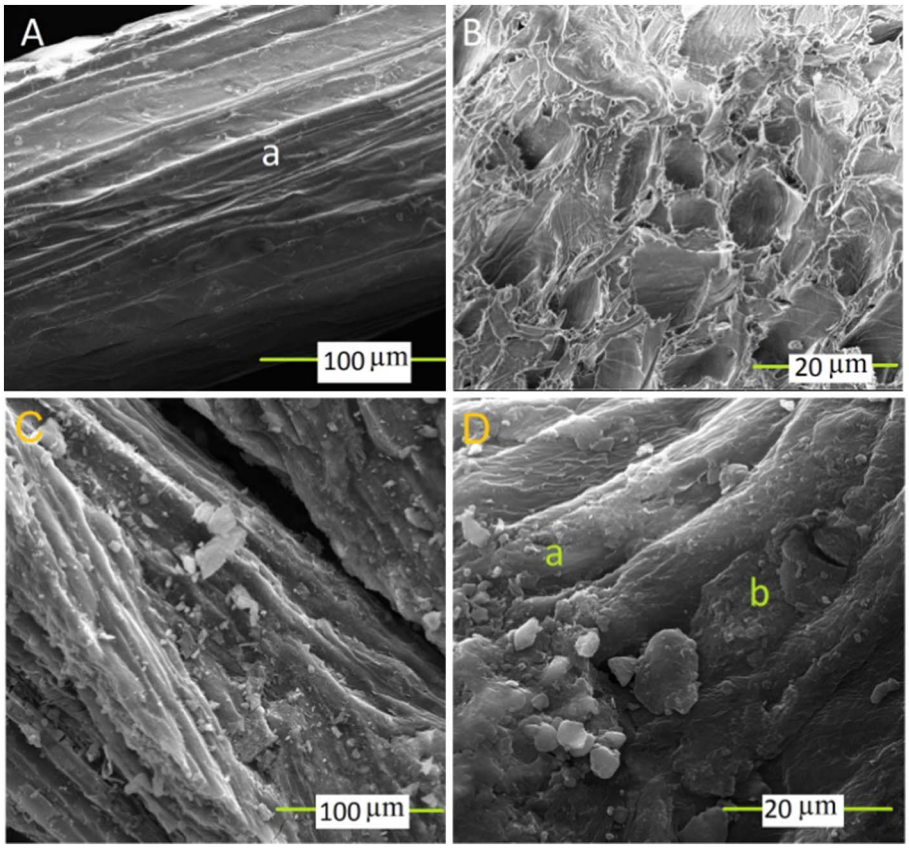

Fig. 3. SEM image of LCF (A), cross-section of one fibre (B), LCF in the geopolymer matrix (C), and LC fibrils (D).

mer matrix is reported in Fig. 5. Metakaolin is shown in Fig. 5A as layers with irregular boundaries due to the calcination of kaolinite at 750 °C. These layers dissolve in the alkaline solution and transform to amorphous geopolymer or microcrystalline gel as illustrated in Fig. 5B and C. The amorphous geopolymer gel acts as a binding material (Alshaaer et al., 2014) (point a). The geopolymer microstructure is characterized by the coexistence of a geopolymer gel (point a) and partially unreacted metakaolinite layers (point b).

According to the SEM images shown in Fig. 5B (SK-geopolymer) and 5C (LG-composite matrix), two microstructural and chemical changes occur in the geopolymer structure as a result of reinforcement with LCF: (1) the unreacted metakaolin (point b) decreases when using LCF, and (2) the geopolymer gel particles (point a) become coarser. These two differences indicate that the geopolymerization reactions are substantially activated by using LCF. The LG-composite microstructure contains less unreacted metakaolin, and much larger geopolymer gel particles. Such an improvement in the geopolymerization reactions is attributed to internal transportation of the alkali solution through the LCF vascular system with 10 µm diameter micro tubes, as shown in Fig. 3B. A good distribution and regular release rate of the alkali solution via the LCF vascular system could enhance the formation of large geopolymer gel particles while consuming the precursors (metakaolin in this case). This is a very important finding calling for further research beyond the approach adopted here.

Two main morphological types of crystalline objects were observed in LG-composite: fibre-like crystals, or whiskers, and fine crystals with a cubic shape, Fig. 6. These crystalline objects are not reported in SK-geopolymer. The SEM analysis of the microstructure of the LG-composite identified the clusters of fibrous crystals or whiskers which radiate out from the centers, reported in Fig. 6A. These crystal clusters grown in a strong geopolymerization alkali environment are composed of well-defined fibres, 100 nm wide and 30 to 40 µm long, and there are

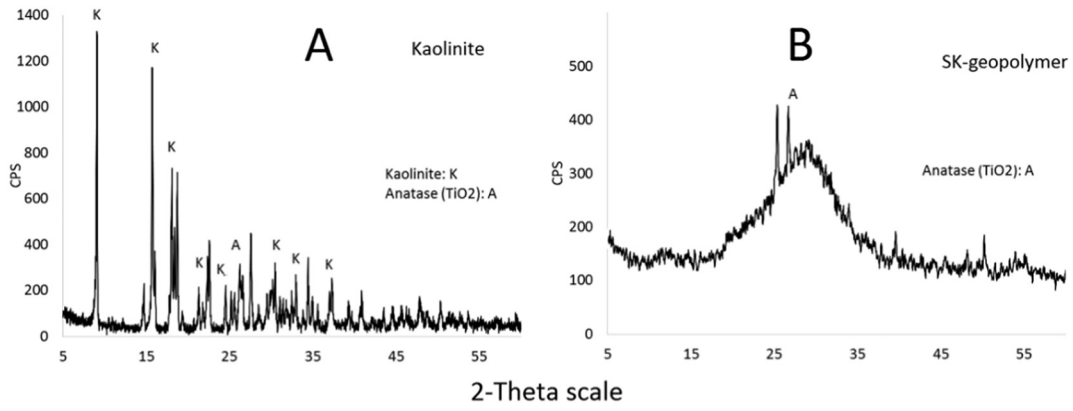

Fig. 4. XRD patterns of kaolinite, and geopolymeric matrix (SK-geopolymer).

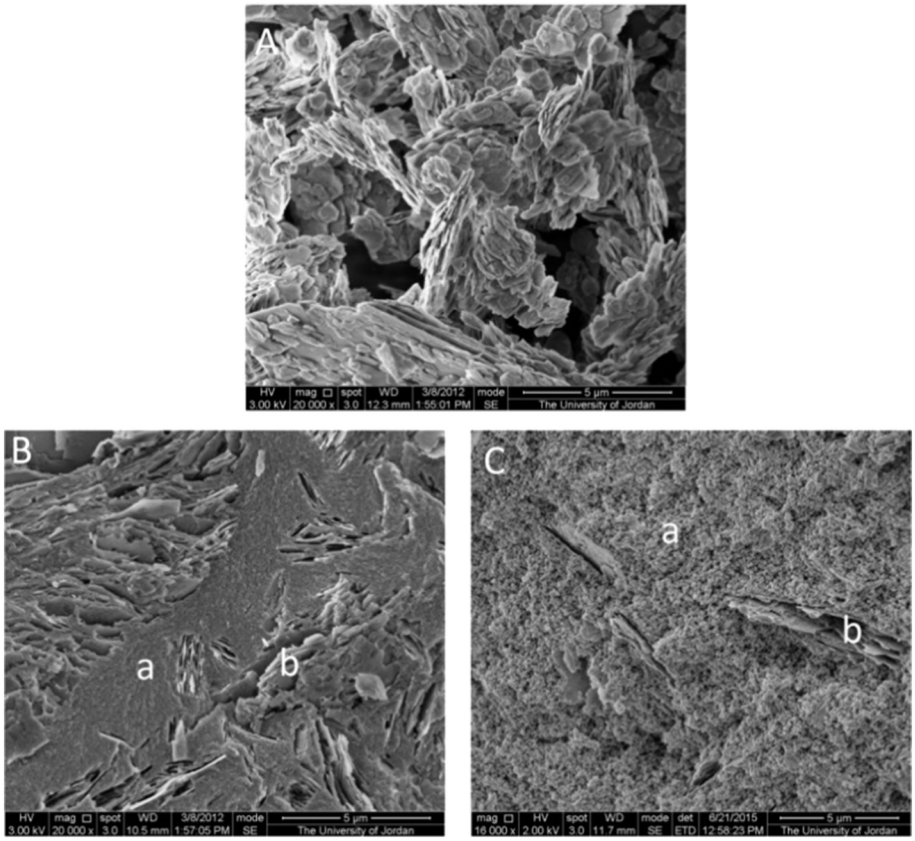

Fig. 5. SEM images taken at the same magnification showing (A) the metakaolin, (B) the SK-geopolymer (SKG), and (C) the geopolymer matrix of LG-composite.

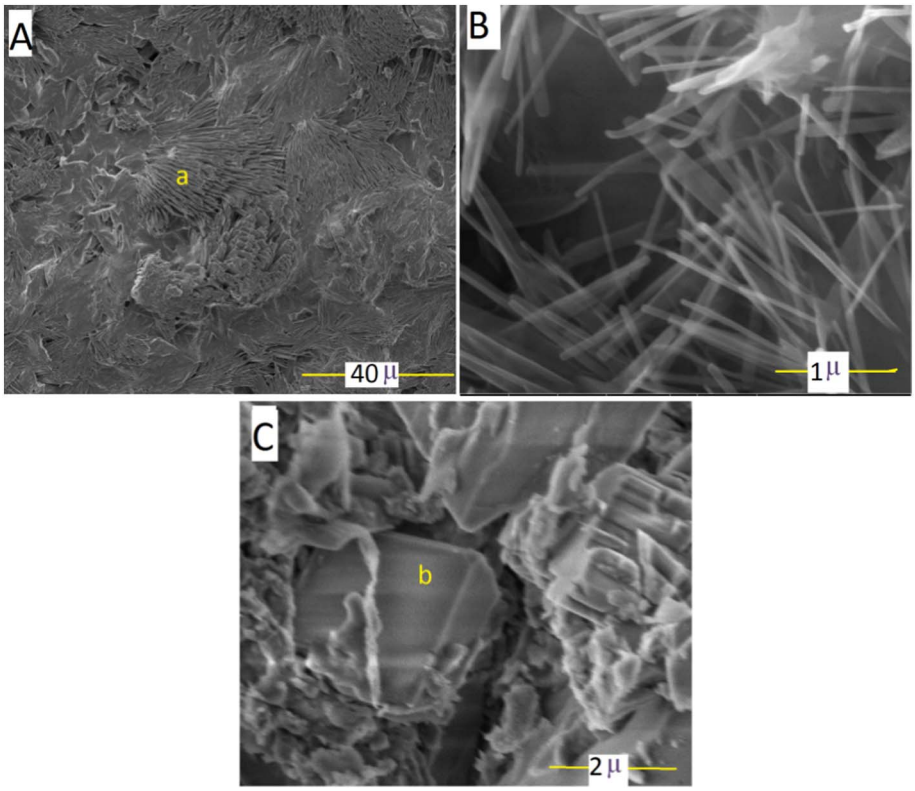

Fig. 6. SEM image of crystalline phases (LG-composite): fibrous (A) and (B), and cubic (C).

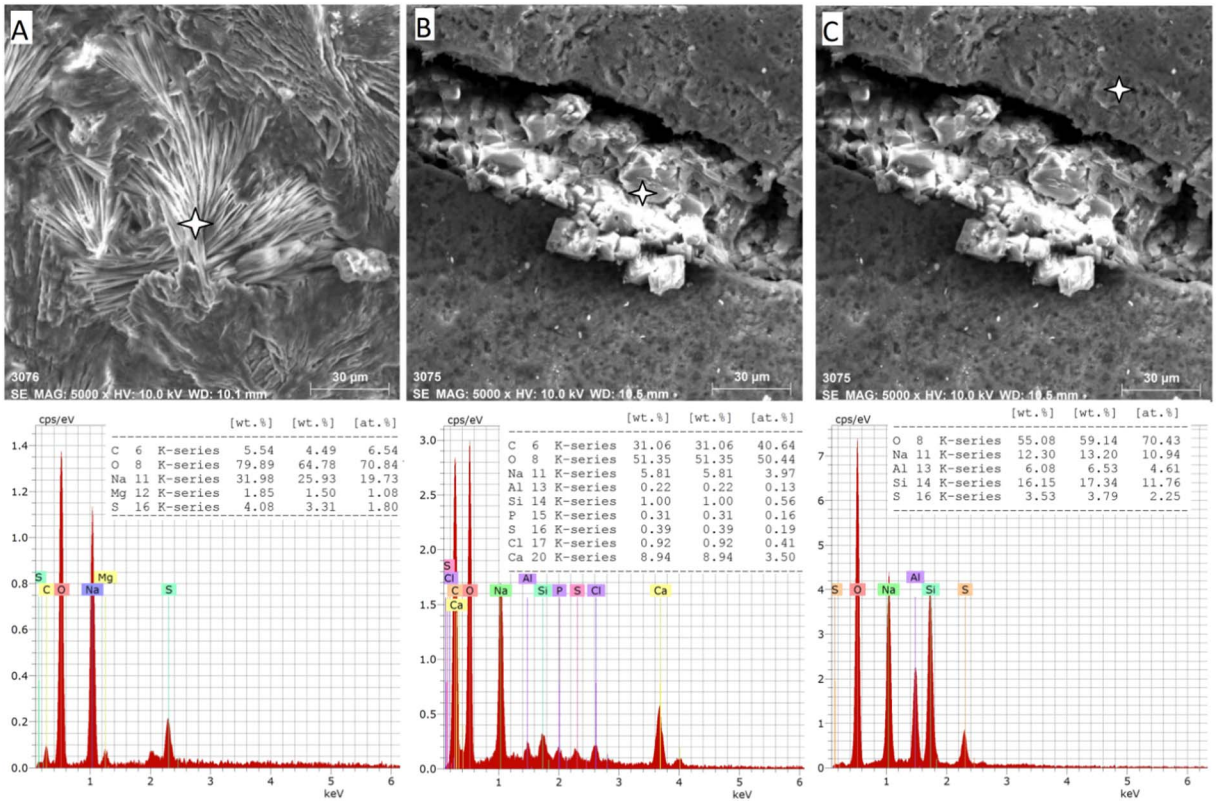

Fig. 7. EDX analysis of LG-composite microstructure; fibrous crystals (A), cubic crystals (B), and the matrix of LG-composite (C).

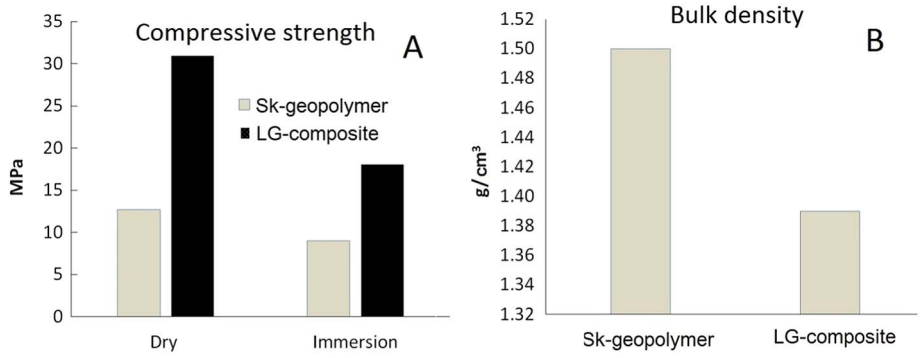

Fig. 8. Compressive strength and bulk density of SK-geopolymer and LG-composite.

clear grain boundaries between individual fibres, Fig. 6B.

The EDX elemental analysis, Fig. 7A, reveals that the fibrous crystals are composed, by atomic percentage, from O (70.84%), Na (19.73%), C (6.54%), and smaller percentages of S (1.80%) and Mg (1.09%). The source of Na is the silicate solution used to prepare the geopolymer matrix, while C, S, and Mg come from LCF (Innocent et al., 2013). The presence of C, S, and Mg in these fibrous crystals confirms the removal of some LCF constituents, i.e. the hemicelluloses and lignin, during the geopolymerization. Therefore, the hydrophobicity of LCF increases and serves to strengthen the bonding between fibre and geopolymer matrix (Joseph et al., 2000). These whiskers could improve a crack-healing ability, as well as increase the fracture toughness and tensile strength (Nevarez-Rascon et al., 2011; Ming et al., 2017).

The other fine cubic crystals of Fig. 7C are observed in LG-composite filling microcracks and voids, as shown in Fig. 7B. The EDX analysis demonstrates that these crystals are composed mainly, in atomic percentages, of C (40.64%), O (50.44), Na (3.97%), Ca (3.50%) and small percentages (less than 1%) of Al, Si, P, S, and Cl. The main difference in chemical composition between this crystal phase and the fibrous crystals is the lower percentage of Na, and the presence of a wide range of chemical elements.

As a result of the growth of crystals in cracks, as in Fig. 7B, the LG-composite exhibits an autogenous healing capacity when moisture and alkaline solution are present in the matrix. When water contacts the residual constituents, further reaction occurs. Moreover, dissolved CO_2 reacts with Na^{1+} to form Na_2CO_3 crystals. These two mechanisms, however, may only heal small cracks. LCFs enhance the healing mechanism: by introducing these fibres in the geopolymer matrix, multiple cracking occurs instead of one wide crack, and these cracks are smaller and close more easily due to autogenous healing.

Finally, The EDX elemental analysis, Fig. 7C, reveals that the amorphous geopolymer matrix in LG-composite is composed of Si (11.76%), Na (10.94%), Al (4.61%), and S (2.25%). Similar to crystal phases, the source of S is the dissolved constituents of LCF, while the other constituents are standard products of geopolymers, but with high deficiency in Al compared to the basic precursors.

3.2. Mechanical and physical properties

The compressive strengths of the SK-geopolymer and LG-composite are given in Fig. 8. Those of LG-composite increase from 13 MPa to 31 MPa, and from 9 MPa to 18 MPa, respectively under dry and immersed conditions. The samples show lower compressive strength after water immersion than in dry conditions (Zhang et al. 2012). This means that the leaching of sodium and hydroxide cations from the binders or pore solution in binders, due to immersion, has some effects on compressive strength development, which means less strength improvement (Zhang et al., 2014). The vascular network system of LCF reinforcement leads to a more homogeneous and slower rate of alkaline solution during the very early period of the setting reactions, and therefore a greater amount of geopolymer gel —the binding material— is produced (Fig. 5). The fibre content and fibre strength are mainly responsible for the strength properties of the LG-composite. A geopolymer sample without LCF generally has cracks that propagate from the centre of the top of the sample and travel in a 45° angle towards the sides of the sample. Samples with LCF limit the propagation of cracks and never fail in an identical way due to the random distribution of the LCF. This also indicates good adhesion between the LCF and geopolymer matrix, and furthermore proves that the LCF did not undergo deterioration under the high alkali environment of geopolymerization. Despite the significant increase in strength of LG-composite compared with the SK-geopolymer matrix, the former exhibits much less bulk density, 1.38 g/cm^3, as opposed to the reference SK-geopolymer, 1.5 g/cm^3. Therefore the LG-composite can be considered to present low weight along with high mechanical performance.

A typical stress-strain curve of LG-composites, with the LCF (10% V/V), was obtained from the Instron machine as shown in Fig. 9. The value of ultimate flexural stress of pure geopolymer matrix (SK-geopolymer) is 3.4 MPa, Fig. 9. But when the matrix is reinforced with LCF that is LG-composite, in the volume percentage 10%, the value of ultimate stress is increased to 14.2 MPa. The tensile strength of natural fibres is more than that of the pure geopolymer matrix, which leads to an observable increase in flexural strength with the incorporation of LCF. The values of ultimate stress and yield stress (Fig. 9) are thus indicative of fibre-matrix adhesion in composites. Flexural strength increased by 4.4 times due to the incorporation of LCF in the composites. Similarly, a 2.4 times enhancement in compressive strength can be observed when LCF are used as reinforcement in the LG-composites as compared to that of the pure SK-geopolymer matrix.

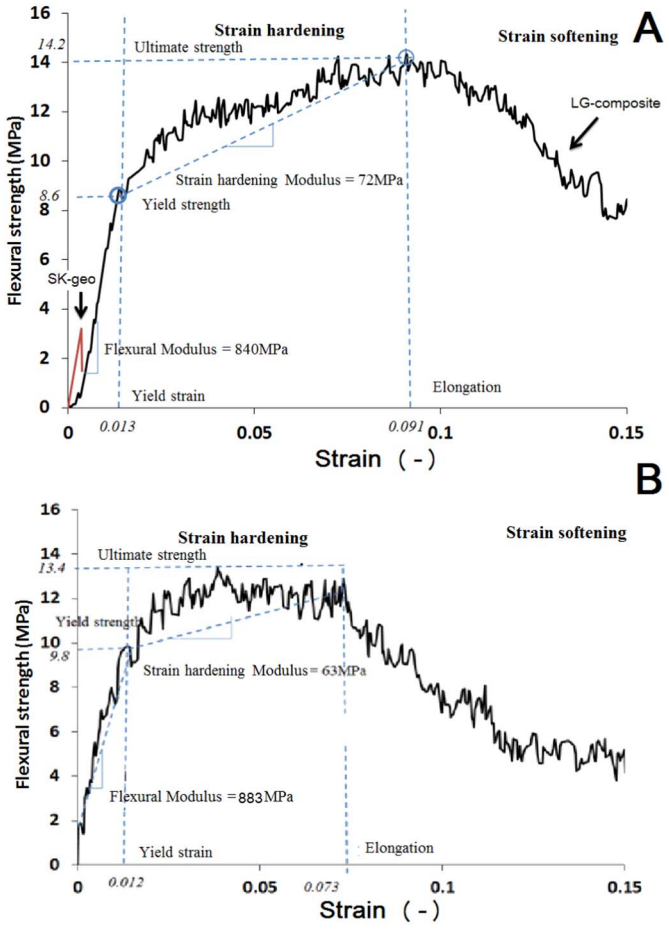

Fig. 9. Typical stress–strain curves of geopolymer composites with the LCF (10% V/V), a specimen non-aged (A), and a specimen aged for 20 months (B).

A pure geopolymer matrix, like other brittle materials, does not have a yield point, and does not strain-harden (Kuenzel et al., 2013). Therefore, the ultimate strength and breaking strength would be the same as shown in Fig. 9. Similar to other composite materials, the overall flexural behavior of LCG can be characterized by a steep elastic region up to yield strength, 8.6 MPa. The ultimate flexural strength of the LG-composite, 14.2 MPa, was reached at the strain of approximately 0.091. Subsequently, a softening of the composite was observed. First cracking occurred at a stress level between 8 and 9 MPa. Distinct multiple crack formation could be seen on specimen surfaces with increasing strain. At the same time, an observable strain hardening of the composite material was recorded with a Modulus of 72 MPa. The failure of the composite was marked by increasing localization of the crack generation, along with the crack widening of one major crack. The widths of cracks outside the major crack plane decreased while tensile stress decreased in the softening regime.

The enhancement of mechanical properties through the introduction of LCF as reinforcement is generally consistent with the behavior of fibre-reinforced composites, and is expected since the strength of such composites is a result of transferring the stress between the LCF and the matrix. The alkaline geopolymer matrix degrades the hemicellulose, pectin, and lignin in the LCF, breaking the fibre bundles and increasing the contact area between the matrix and fibres, resulting in the ductile failure behavior (Alzeer and MacKenzie, 2012) indicated in Fig. 3. The LCF had a maximum flexural strength of 17.08 MPa (Ubi and Asipita, 2015). Therefore, the LCF-reinforced composite provides an acceptable alkaline environment for these fibres, retaining most of their strength after geopolymerization. Fig. 9A illustrates that the value of flexural modulus of the matrix (SKG) is 914 MPa. When the composites are formed with untreated LCF, the elastic modulus decreases slightly to a value of 840 MPa in LGC. However, the ductile behavior of the composites is an obvious result of LCF incorporation.

In composites, interfacial adhesion between the reinforcement and the matrix is usually weak as a result of the hydrophilic nature of the fibre and the hydrophobic nature of the matrix, hence the need for chemical modification of the fibre surfaces (Mohsen and El-maghraby, 2010). The initial high alkalinity of the geopolymer paste causes mercerization of LCF, as reflected in Fig. 3D. This treatment reduces the moisture absorption, and increases the wettability characteristics that enhance the mechanical properties of composites (Rozman et al., 2000; Mohd et al., 2012). Chemical modification of the luffa fibres enhances the flexural strength and modulus of composites; and appropriate alkali treatment is a key technology for improving mechanical properties of LC-based fibre composites (Holbery and Houston, 2006; Davoodi et al., 2010).

These luffa fibres exhibit a maximum flexural strength of 17 MPa. Results obtained in the research (Ubi and Asipita, 2015) show that NaOH treatment may improve the mechanical properties of LCF. That is, the geopolymer alkaline environment during the setting reactions does not deteriorate these fibres. The SEM image of Fig. 3C shows the LCF to exhibit a limited chemical attack (point c) as a result of geopolymerization reactions. A strong adhesion between the geopolymer gel and the fibre surface are reflected in Fig. 3C (point b). Finally

the chemical treatment on LCF causes fibrillation of fibre to small fibrils. With the decrease in fibre diameter, the surface area increases, thereby favoring the wettability of fibres within the matrix. The high interfacial area is the most beneficial aspect of composites with treated fibres (Alshaaer et al., 2002).

In addition to the mechanical effect, the well-organized vascular networking system of these fibres could play an essential rule in distributing the alkaline solution during setting reactions, possibly improving the microstructure by forming a denser binding material (geopolymer gel). Not only does the LCF have physical (mechanical) effects —there is also a potential chemical influence on the geopolymer matrix.

A preliminary study of aging effects was investigated by 3-point bending tests, where samples aged for 20 months at ambient conditions as illustrated in Fig. 9. The flexural yield strength of LG-composite increases with the aging time of 20 months, from 8.6 MPa (Fig. 9A) to 9.8 MPa (Fig. 9B). This increment in yield strength is because of the geopolymerization process of geopolymer with aging. Slight changes occur on ultimate flexural strength, strain hardening, and flexural modulus over 20 months of aging. This preliminary aging study has demonstrated that the LG-composite shows no significant deterioration in mechanical performance over a duration of 20 months.

4. Conclusions

This work reports on new “green” composites of geopolymer reinforced with 10 vol% Luffa Cylindical Fibres (LCF) to produce materials with excellent mechanical and physical properties.

When LCF are subjected to a strongly alkali geopolymerization environment, the wax, fatty acids, hemicellulose, and lignin are removed. Removal of these substances results in a rough surface with pits, which leads to an increase in mechanical interlocking between treated LCF and matrix. The strong alkali geopolymerization causes fibrillation of fibre to small fibrils. With the decrease in fibre diameter, surface area increases, hence greater wettability of fibres within the matrix. Two main morphological types of crystalline objects were observed in LG-composite due to the incorporation of the extracted constituents of LCF: fibre-like crystals, or whiskers, and fine crystals with a cubic shape. These crystals could assist in crack healing, increasing the tensile strength and toughness of the composite. Analysis using SEM confirms that the LF- geopolymer composite produces higher amounts of geopolymer gel. The addition of LF-composite provides for a denser microstructure, and coarser geopolymer gel particles. A substantial enhancement of flexural strength (from about 3.4 MPa to about 13.2 MPa) was obtained with LCF reinforcement. The alkaline matrix increases the contact area between the matrix and fibres, resulting in ductile failure behavior (Zhao et al., 2016). The mechanical properties of the LF fibre do not appear to be degraded by the alkaline conditions of the geopolymer synthesis. It was also observed that the LG-composite reduced overall bulk density while increasing flexural and compressive strength. The LCF-reinforced geopolymer composite exhibits ductile-like failure with a strain hardening Modulus of 72 MPa, unlike the brittle matrix. A preliminary aging study has demonstrated that the LG-composite shows no significant deterioration in mechanical performance over a duration of 20 months.

Acknowledgments

The financial support of the project “Development of functional geopolymer-based construction materials for passive cooling of buildings” funded under the contract number (AT-34-211) by the King Abdulaziz City for Science and Technology KACST, within the Research Grants Program, is gratefully acknowledged.

#References

Akhtar, N., Saeed, A., Iqbal, M., 2003. *Chlorella sorokiniana* immobilized on the biomatrix of vegetable sponge of *Luffa cylindrica*: a new system to remove cadmium from contaminated aqueous medium. Bioresour. Technol. 88 (2), 163–165.

Alomayri, T., Shaikh, F.U.A., Low, I.M., 2013. Characterisation of cotton fibre-reinforced geopolymer composites. Compos. Part B 50, 1–6.

Alomayri, T., Shaikh, F.U.A., Low, I.M., 2014. Synthesis and mechanical properties of cotton fabric reinforced geopolymer composites. Compos. Part B 60, 36–42.

Alshaaer, M., 2013. Two-phase geopolymerization of kaolinite-based geopolymers. Appl. Clay Sci. 86, 162–168.

Alshaaer, M., Cuypers, H., Wastiels, J., 2002. Stabilisation of kaolinitic soil for construction purposes by using mineral polymerisation technique. In: Resheidat, Musa (Ed.), Proceedings of the 6th International Conference Technology for Developing Countries. vol.3. pp. 1085–1092. Jordan, https://books.google.com.sa/books/about/Proceedings_of_the_6th_International_Con.html?id=0m2cmwEACAAJ&redir_esc=y.

Alshaaer, M., Zaharaki, D., Komnitsas, K., 2014. Microstructural characteristics and adsorption potential of a zeolitic tuff–metakaolin geopolymer. Desalin. Water Treathttp://dx.doi.org/10.1080/19443994.2014.938306.

Alzeer, M., MacKenzie, K.J.D., 2012. Synthesis and mechanical properties of new fibre-reinforced composites of inorganic polymers with natural wool fibres. J. Mater. Sci. 47, 6958–6965.

Alzeer, M., MacKenzie, K.J.D., 2013. Synthesis and mechanical properties of novel composites of inorganic polymers (geopolymers) with unidirectional natural flax fibres. Appl. Clay Sci. 75–6, 148–152.

Assaedi, H., Shaikh, F.U.A., Low, I.M., 2015. Utilization of nanoclay to reinforce flax fabric-geopolymer composites. Int. J. Chem. Mol. Nucl. Mater. Metall. Eng. 9 (12), 1331–1339.

Assaedi, H., Shaikh, F.U.A., Low, I.M., 2016. Characterizations of flax fabric reinforced nano-clay-geopolymer composites. Compos. B 95, 412–422.

Barbosa, V.F.F., MacKenzie, K.J.D., Thaumaturgo, C., 2000. Synthesis and characterisation of materials based on inorganic polymers of alumina and silica: sodium polysialate polymers. Int. J. Inorg. Mater. 2 (4), 309–317.

Bohlooli, H., Nazari, A., Khalaj, G., Kaykha, M.M., Riahi, S., 2012. Experimental investigations and fuzzy logic modeling of compressive strength of geopolymers with seeded fly ash and rice husk bark ash. Compos. Part B 43 (3), 1293–1301.

Davidovits, J., 2015. False Values on CO2 Emission For Geopolymer Cement/Concrete Published in Scientific Papers. Technical Paper #24 Geopolymer Institute Library. www.geopolymer.org.

Davidovits, J., 2011. Chapter 21: geopolymer fiber-composites. In: Geopolymer Chemistry and Applications. Geopolymer Institute (ISBN 9782951482098).

Davidovits, J., 1982. Mineral polymers and methods of making them. US Patent No 44721993.

Davidovits, J., 2005. Geopolymer chemistry and sustainable development. The poly (sialate) terminology: a very useful and simple model for the promotion and understanding of green-chemistry. In: Davidovits, J. (Ed.), Proc. of the World Congress Geopolymer, Saint Quentin, France, pp. 9–15 28 June–1 July 2005.

Davoodi, M.M., Sapuan, S.M., Ahmad, D., Aidy, D., Khalina, A., Mehdi, J., 2010. Mechanical properties of hybrid kenaf/glass reinforced epoxy composite for passenger car bumper beam. Mater. Des. 31, 4927–4932.

Duxson, P., Fernandez-Jimenez, A., Provis, J.L., Luckey, G.C., Palomo, A., van Deventer, J.S.J., 2007. Geopolymer technology: the current state of the art. J. Mater. Sci. 42, 2917–2933.

El-Eswed, B., Aldagag, O.M., Khalili, F., 2017. Efficiency and mechanism of stabilization/solidification of Pb(II), Cd(II), Cu(II), Th(IV) and U(VI) in metakaolin based geopolymers. Appl. Clay Sci. 140, 148–156. http://dx.doi.org/10.1016/j.clay.2017.02.003.

El-Eswed, B., Yousef, R.I., Alshaaer, M., Khalili, F., Khoury, H., 2009. Alkali solid-state conversion of kaolin and zeolite to effective adsorbents for removal of lead from aqueous solution. Desalin. Water Treat. 8, 124–130.

Essaidi, N., Samet, B., Baklouti, S., Rossignol, S., 2014. Feasibility of producing geopolymers from two different Tunisian clays before and after calcination at various temperatures. Appl. Clay Sci. 88–89, 221–227.

Ferreira, J.A.M., Capela, C., Costa, J.D., 2010. A study of the mechanical properties of natural fibre reinforced composites. Fibers Polym. 11 (8), 1181–1186.

Gianpietro, V., Amaducci, S., Vannini, L., 2000. Multi-use Crops, Programme by DG XII of the European Commission. Department of Agronomy, University Bolognapp. 82–83.

Hajjaji, W., Andrejkovičová, S., Zanelli, C., Alshaaer, M., Dondi, M., Labrincha, J.A., Rocha, F., 2013. Composition and technological properties of geopolymers based on metakaolin and red mud. Mater. Des. 52, 648–654.

Hammell, J.A., Balaguru, P.N., Lyon, R.E., 2000. Strength retention of fire resistant aluminosilicate–carbon composites under wet–dry conditions. Compos. Part B 31, 107–111.

Holbery, J., Houston, D., 2006. Natural fibre reinforced polymer composites in automotive applications. J. Miner. Met. Mater. Soc. 58, 80–86.

Hung, T.D., Pernica, D., Kroisová, D., Bortnovsky, O., Louda, P., Rylichova, V., 2008. Composites based on geopolymer matrices: preliminary fabrication, mechanical properties and future applications. Adv. Mater. Res. 55–57, 477–480.

Huntzinger, D.N., Eatmon, T.D., 2009. A life-cycle assessment of Portland cement manufacturing: comparing the traditional process with alternative technologies. J. Clean. Prod. 17 (7), 668–675. http://dx.doi.org/10.1016/j.jclepro.2008.04.007.

Innocent, O., Oboh, Emmanuel, Aluyor, O., Thomas, O.K., Audu, 2013. Mathematical and ANN models of the effect of dosage on Cu^{2+} sorption capacity of Luffa Cylindrica. Solids Struct. (SAS) 2 (2).

Joseph, K., Mattoso, L.H.C., Toledo, R.D., Thomas, S., Carvalho, L.H., de Pothen, L., Kala, S., James, B., Frollini, E., 2000. Natural fiber reinforced thermoplastic composites. In: Leão, A.L., Mattoso, L.H.C. (Eds.), Natural Polymers and Agrofibers Composites. Embrapa, USP-IQSC, UNESP, São Carlos, Brazil, pp. 159–201.

Komnitsas, K., Zaharaki, D., Bartzas, G., 2013. Effect of sulphate and nitrate anions on heavy metal immobilisation in ferronickel slag geopolymers. Appl. Clay Sci. 73, 103–109.

Komnitsas, K., Zaharaki, D., Perdikatsis, V., 2007. Geopolymerisation of low calcium ferronickel slags. J. Mater. Sci. 42 (9), 3073–3082.

Kriven, W.M., Bell, J.L., Gordon, M., 2003. Microstructure and microchemistry of fully-reacted geopolymers and geopolymer matrix composites. Ceram. Trans. 153 (4), 227–250.

Kuenzel, C., Neville, T.P., Donatello, S., Vandeperre, L., Boccaccini, A.R., Cheeseman, C.R., 2013. Influence of metakaolin characteristics on the mechanical properties of geopolymers. Appl. Clay Sci. 83–84, 308–314.

Low, I.M., Somers, J., Kho, H.S., Davies, I.J., Latella, B.A., 2009. Fabrication and properties of recycled cellulose fibre-reinforced epoxy composites. Compos. Interfaces 16, 659–669.

MacKenzie, K.J.D., Welter, M., 2014. Geopolymer (aluminosilicate) Composites: Synthesis, Properties and Applications. Victoria University of Wellington, New Zealand.

Ming, L., Shuang, D., Yongjin, Y., Jianzhou, J., Yujia, Y., Xiaoyang, G., 2017. Mechanical properties and microstructure of oil well cement stone enhanced with Tetra-needle like ZnO whiskers. Constr. Build. Mater. 135, 59–67.

Mohd, Y.H., Mohd, N.R., Azriszul, M.A., Ahmad, M.A.Z., Saparudin, A., 2012. Mercerisation treatment parameter effect on natural fibre reinforced polymer matrix composite: a brief review. World Acad. Sci. Eng. Technol. 6, 1378–1384.

Mohsen, Q., El-maghraby, A., 2010. Characterization and assessment of Saudi clays raw material at different area. Arab. J. Chem. 3, 271–277.

NagarajaGanesh, B., Muralikannan, R., 2016. Comprehensive characterization of lignocellulosic fruit fibers reinforced hybrid polyester composites. Compos. Mater. 1 (1), 1–6. http://dx.doi.org/10.11648/j.cm.20160101.11.

Nematollahi, B., Sanjayan, J., Shaikh, F.U.A., 2014. Comparative deflection hardening behavior of short fiber reinforced geopolymer composites. Constr. Build. Mater. 70, 54–64.

Nevarez-Rascon, A., Aguilar-Elguezabal, A., Orrantia, E., Bocanegra-Bernal, M.H., 2011. Compressive strength, hardness and fracture toughness of Al_2O_3 whiskers reinforced ZTA and ATZ nanocomposites: Weibull analysis. Int. J. Refract. Met. Hard Mater. 29, 333–340.

Parida, C., Dash, S.K., Das, S.C., 2015. Effect of fiber treatment and fiber loading on mechanical properties of luffa-resorcinol composites. Indian J. Mater. Sci. 2015, 658064. http://dx.doi.org/10.1155/2015/658064.

Pernica, D., Reis, P., Ferreira, J., Louda, P., 2010. Effect of test conditions on the bending strength of a geopolymer-reinforced composite. J. Mater. Sci. 45, 744–749.

Rahman, M.M., Rashid, M.H., Hossain, M.A., Hasan, M.T., Hasan, M.K., 2011. Performance evaluation of bamboo reinforced concrete beam. Int. J. Eng. Technol. IJET IJENS 11 (04), 113–118.

Ray, D., Sarkar, B.K., Rana, A.K., Bose, N.R., 2001. Effect of alkali treated jute fibres on composite properties. Bull. Mater. Sci. 24 (2), 129–135.

Roy, D.M., 1999. Alkali-activated cements, opportunities and challenges. Cem. Concr. Res. 29 (2), 249–254.

Rozman, H.D., Lai, C.Y., Ismail, H., Mohd Ishak, Z.A., 2000. The effect of coupling agents on the mechanical and physical properties of oil palm empty fruit bunch polypropylene composites. Polym. Int. (49), 1273–1278.

Seki, Y., Sever, K., Erden, S., Sarikanat, M., Neser, G., Ozes, C., 2012. Characterization of *Luffa cylindrica* fibers and the effect of water aging on the mechanical properties of its composite with polyester. J. Appl. Polym. Sci. 123 (4). http://dx.doi.org/10.1002/app.34744.

Ubi, P.A., Asipita, S.A., 2015. Effect of sodium hydroxide treatment on the mechanical properties of crushed and uncrushed *luffa cylindrica* fibre reinforced rldpe composites. Int. J. Chem. Mol. Nucl. Mater. Metall. Eng. 9 (1), 203–208.

Zaharaki, D., Komnitsas, K., Perdikatsis, V., 2010. Use of analytical techniques for identification of inorganic polymer gel composition. J. Mater. Sci. 45 (10), 2715–2724.

Zhang, Z.H., Yang, T., Wang, H., 2014. The effect of efflorescence on the mechanical properties of fly ash-based geopolymer binders. In: Smith, S.T. (Ed.), 3rd Australasian Conference on the Mechanics of Structures and Materials (ACMSM23) Byron Bay, Australia, 9-12 December 2014.

Zhang, Z., Yao, X., Wang, H., 2012. Potential application of geopolymers as protection coatings for marine concrete III. Field experiment. Appl. Clay Sci. 67–68, 57–60.

Zhao, W., Wang, Y., Wang, X., Wu, D., 2016. Fabrication, mechanical performance and tribological behaviors of polyacetal-fiber-reinforced metakaolin-based geopolymeric composites. Ceram. Int. 42, 6329–6341.